Energy Transfer Hot Paper

Deutsche Ausgabe: DOI: 10.1002/ange.201600428
Internationale Ausgabe: DOI: 10.1002/anie.201600428

Non-Radiative Energy Transfer Mediated by Hybrid Light-Matter States

*Xiaolan Zhong, Thibault Chervy, Shaojun Wang, Jino George, Anoop Thomas, James A. Hutchison, Eloise Devaux, Cyriaque Genet, and Thomas W. Ebbesen**

Abstract: *We present direct evidence of enhanced non-radiative energy transfer between two J-aggregated cyanine dyes strongly coupled to the vacuum field of a cavity. Excitation spectroscopy and femtosecond pump–probe measurements show that the energy transfer is highly efficient when both the donor and acceptor form light-matter hybrid states with the vacuum field. The rate of energy transfer is increased by a factor of seven under those conditions as compared to the normal situation outside the cavity, with a corresponding effect on the energy transfer efficiency. The delocalized hybrid states connect the donor and acceptor molecules and clearly play the role of a bridge to enhance the rate of energy transfer. This finding has fundamental implications for coherent energy transport and light-energy harvesting.*

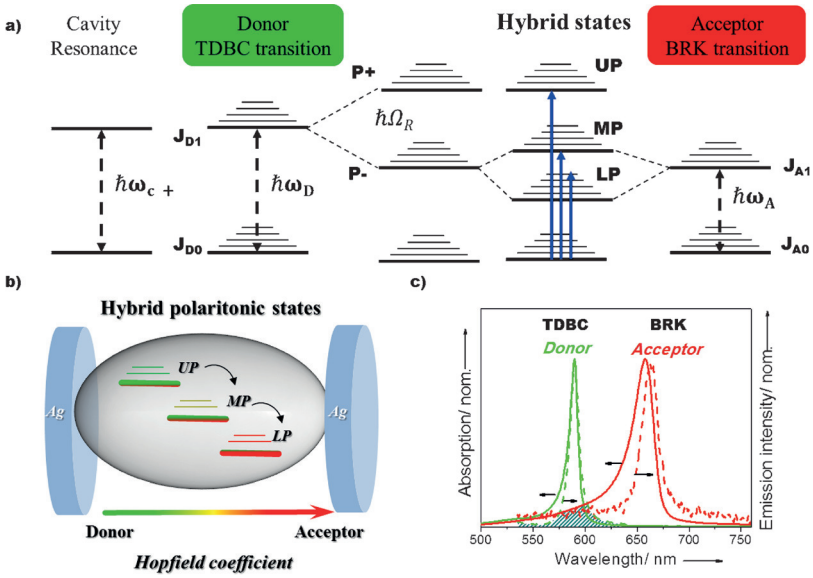

Figure 1. a) Schematic representation of strong coupling successively with the donor resonant with a cavity mode $\hbar\omega_c$, and then the acceptor, leading to the formation of three new eigen hybrid light-matter states: the upper (UP), middle (MP), and lower (LP), polaritonic states. P+ and P− are the polaritonic states separated by the Rabi splitting energy $\hbar\Omega_R$ when the cavity is just coupled to the donor. b) Schematic diagram of the different donor and acceptor contents (Hopfield coefficient) of UP, MP, and LP states in the strongly coupled cavity with UP having the largest donor character while LP is mostly acceptor-like. c) Normalized spectroscopic data for the donor and acceptor materials. The green solid and dash curves are the TDBC absorption and emission spectra on top of a 30 nm Ag film, while the red solid and dash curves are for the BRK acceptor. The shadowed part is the overlap between the donor emission and acceptor absorption spectra.

When an exciton transition and a resonant optical mode exchange energy faster than any competing dissipation process, it can lead to light-matter strong coupling and the generation of two new hybrid (polaritonic) eigenstates, P+ and P−, separated by the so-called Rabi splitting (Figure 1a). This brings about interesting properties possessed by neither the original exciton or the optical mode,[1–19] and leads to new possibilities, such as modified chemical reactivity,[5,6] and enhanced conductivity of organic semiconductors.[9] In the latter case, the enhancement stems from the delocalized nature of the hybrid states over the spatial extent of the optical mode[10,11] which is expected to affect energy transport according to recent theoretical studies.[12,13]

In this context, it is interesting to consider how such hybrid states would affect energy transfer between donor and acceptor molecules. Energy transfer is a non-radiative process which has been extensively studied over the last century and typically involves either Coulombic interactions (Förster) or electronic exchange (Dexter).[20] A key confirmation of energy transfer is of course a reduction in the lifetime of the donor concomitant with the rise of the acceptor excited state population. Other factors that affect energy transfer include molecular aggregation, the presence of bridges between the donor and acceptor, and the density of optical states.[20–25] Strong coupling could provide an alternate effective path for energy transfer in analogy with chemically bridged donors and acceptors where the linker mediates the interactions by an effective overlap between the wave functions of both the donor and the acceptor. In the strong coupling case, it is the polaritonic states which are by construction either donor or acceptor-like that mediates the interactions in the system due to their delocalized nature. Recently, energy transfer under strong coupling based on steady-state fluorescence excitation spectroscopy of the acceptor was studied.[17] However no

[*] Dr. X. Zhong, T. Chervy, Dr. S. Wang, Dr. J. George, Dr. A. Thomas, Dr. J. A. Hutchison, Dr. E. Devaux, Dr. C. Genet, Prof. T. W. Ebbesen
ISIS & icFRC
University of Strasbourg and CNRS
8 allée Gaspard Monge, Strasbourg 67000 (France)
E-mail: ebbesen@unistra.fr

Supporting information for this article can be found under: http://dx.doi.org/10.1002/anie.201600428.

change in donor lifetime was reported as would have been expected for non-radiative energy transfer. Indeed the study of energy transfer in cavities is complicated by the fact that the excitation spectra are modulated by the optical mode structure because the transmission peaks of the coupled system overlap with the absorption peaks of the hybrid states.[19]

Herein, we present direct evidence, including transient dynamics, of non-radiative energy transfer in a system in which both the donor and acceptor are simultaneously strongly coupled to an optical cavity. This system gives rise to three new eigenstates, namely the upper (UP), middle (MP), and lower (LP) polaritonic states[26–28] as illustrated in Figure 1 a. It is important to note these states have different donor and acceptor content (Hopfield coefficient), with UP having the largest donor character while LP is mostly acceptor-like as illustrated in Figure 1 b. As a result the energy should flow from UP to LP, again akin to the energy transfer in chemically linked donor–acceptor systems.[21] For the purpose of this study, we used the J-aggregates of two cyanine dyes, TDBC as donor, and BRK as acceptor (see Methods section in the Supporting Information). These J-aggregates are characterized by intense and narrow J-bands and furthermore the TDBC emission spectrum and the BRK absorption spectrum overlap as shown in Figure 1 c.

To build the hybrid light-matter states with TDBC and BRK as illustrated in Figure 1 a, an optical cavity mode is first chosen to be resonant with the TDBC J-aggregate absorption maximum at 590 nm (2.1 eV). In the absence of the acceptor, the absorption spectrum is strongly modified with two new peaks P+ at 549 nm (2.27 eV) and P− at 637 nm (1.95 eV), separated in this case by a Rabi splitting of 320 meV, as shown in Figure 2 a. Note that the P− energy is close to BRK J-aggregate absorption maximum at 659 nm (1.88 eV), hence they in turn can couple, leading to the three hybrid polaritonic eigenstates UP, MP, and LP, illustrated in Figure 1 a and shown experimentally in Figure 2 a for different BRK concentrations.

A crucial factor for Förster-type energy transfer is the average donor–acceptor distance and therefore the relative donor and acceptor concentrations in the sample. Figure 2 a shows absorption spectra of the strongly coupled system with different weight ratios of the donor and the acceptor, from 1:0 to 1:1 in the polyvinyl alcohol, PVA, matrix. These weight ratios are approximately equal to molecular population ratios since the molecular weights of the two molecules are nearly equal (see Supporting Information). The corresponding transmission (T) and reflection (R) spectra are shown in Supporting Information Figure S1. It can be seen that increasing the BRK concentration leads to changes in the position of the MP and LP absorption bands as would expected since strong coupling depends on the square root of the concentration of the molecules involved, that is, here the acceptor.[6]

The above polaritonic state energies can be understood by consideration of a three-coupled oscillator model composed

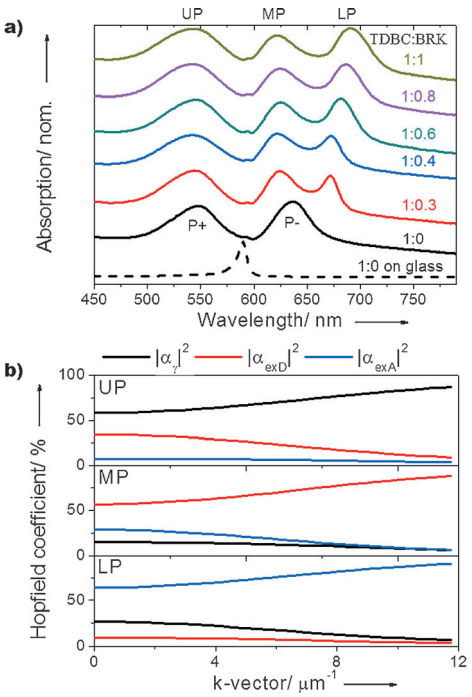

Figure 2. a) Normalized absorption spectra for various weight ratios (1:0 to 1:1) of donor (TDBC) and acceptor (BRK) in the strongly coupled cavity. The absorption A is determined after recording the transmission T and the reflection R of the samples ($A=1-T-R$). The black dash curve shows the donor absorbance spectrum on top of a glass substrate. b) Hopfield coefficient for hybrid light-matter states for the 1:1 donor–acceptor ratio in the strongly coupled system calculated from Equation (1).

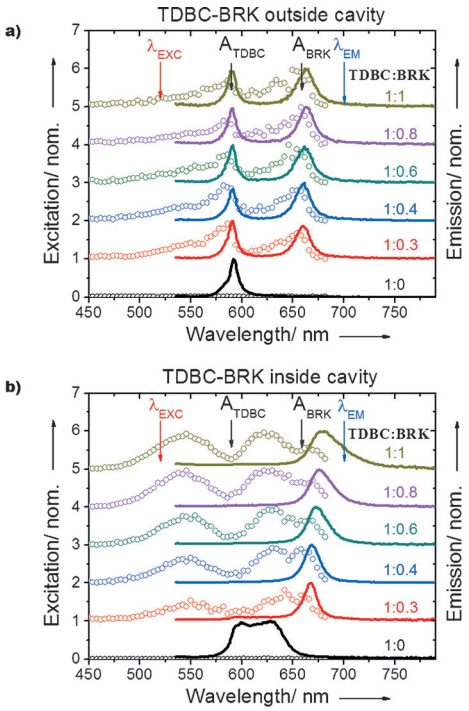

Figure 3. Normalized excitation and emission spectra from varying weight ratios between donor and acceptor. a) in the absence of the top Ag mirror (outside cavity) and b) in the strongly coupled system. The emission spectra are recorded upon excitation at 520 nm while the excitation spectra are collected at 700 nm.

of the optical cavity mode and the two excitonic states of the donor and the acceptor.[17,26–28] The corresponding interaction Hamiltonian is given in the Supporting Information Equation (S1). From this analysis, the mixing coefficients $|\alpha_\gamma|^2$, $|\alpha_{exD}|^2$ and $|\alpha_{exA}|^2$ describe the photonic, donor and acceptor excitonic content of the polaritonic states, known as the Hopfield coefficients, can be estimated. Figure 2b gives these Hopfield coefficients for the 1:1 donor–acceptor strongly coupled cavity as a function of the k-vector (momentum). At optimal coupling ($k=0$), it can be seen that donor/acceptor ratio is the highest in UP ($\alpha|_{exD}|^2/\alpha|_{exA}|^2=7.3$), decreasing in MP ($\alpha|_{exD}|^2/\alpha|_{exA}|^2=2.0$) while LP is dominated by the acceptor ($\alpha|_{exD}|^2/\alpha|_{exA}|^2=0.1$). The photonic content also varies between the three states but it is less pertinent for this study. The value for $\hbar\omega_D$ is 277 meV while $\hbar\omega_A$ varies from 150 meV for the 1:0.3 sample to 200 meV for the 1:1 sample [Eq. (S1) in the Supporting Information]. These hybrid polaritonic states result in complex multibranch energy–momentum dispersion curves shown in Figures S2a and S2b.

In Figure 3a,b, the emission and excitation spectra of the donor–acceptor system under strong coupling are compared with those outside the cavity for the different donor to acceptor ratios. In the absence of the acceptor, the emission of the donor is already modified in the cavity by strong coupling (black curves). The original TDBC fluorescence spectrum at approximately 590 nm is broadened by the new emission at around 637 nm from P–. It should be noted that not all molecules are coupled to the cavity which is mostly due to their orientation and position relative to the optical field[4,19] and hence the mixed emission which disperses (Figure S2c).

In the presence of the acceptor, the emission inside and outside the cavity are remarkably different. Under strong coupling, the emission spectra are dominated by a single peak which corresponds to the LP emission while outside the cavity both TDBC and BRK emission are observed. This change under strong coupling already suggests enhanced energy transfer under strong coupling. An example of the dispersion curves of the emission spectra for donor–acceptor inside the cavity is shown in Figure S2d. To understand these results, we recorded the excitation spectra at 700 nm.

Outside the cavity, the excitation spectra exhibit two components as shown in Figure 3a: one corresponding to the acceptor BRK and the other to the donor TDBC. The one from the TDBC donor is due to the energy transfer from TDBC to BRK since in the absence of the acceptor, the excitation spectra recorded at 700 nm is flat, showing no features (black circles, bottom curves in Figure 3a,b). In the donor–acceptor strongly coupled cavity, the excitation spectra exhibit three peaks corresponding to UP, MP, and LP which shift as the BRK concentration increases in agreement with the absorption peaks of the coupled systems shown in Figure 2a.

These findings suggest energy transfer mediated by the hybrid polaritonic states, however it does not constitute a proof, as discussed earlier. To demonstrate that system is truly undergoing enhanced non-radiative energy transfer under strong coupling, the dynamics of the system was studied by femtosecond transient transmission spectroscopy. The transient spectra recorded for the donor–acceptor inside/outside the cavity are shown in Figure 4a upon 150 fs pulsed excitation at 530 nm. The lifetimes of the transient spectra are shown in Figure 4b where the decay dynamics of donor–acceptor system outside the cavity (black solid circle, Figure 4b) is shown along with the strongly coupled system (red solid circle, Figure 4b). Control experiments involving just the donor show a long lifetime (ca. $\tau_D=12$ ps) whether inside or outside the cavity (same color code but open circles) in agreement with earlier work which has shown that the lifetime of P– is similar to bare excited state lifetime.[4,6] However, in the presence of the acceptor, the decay lifetime in the spectral region of the donor state decreases to $\tau_{DA}=5.5$ ps outside the cavity and to $\tau_{DA}=1.2$ ps in strongly coupled system (Figure 4b). From these values, the energy

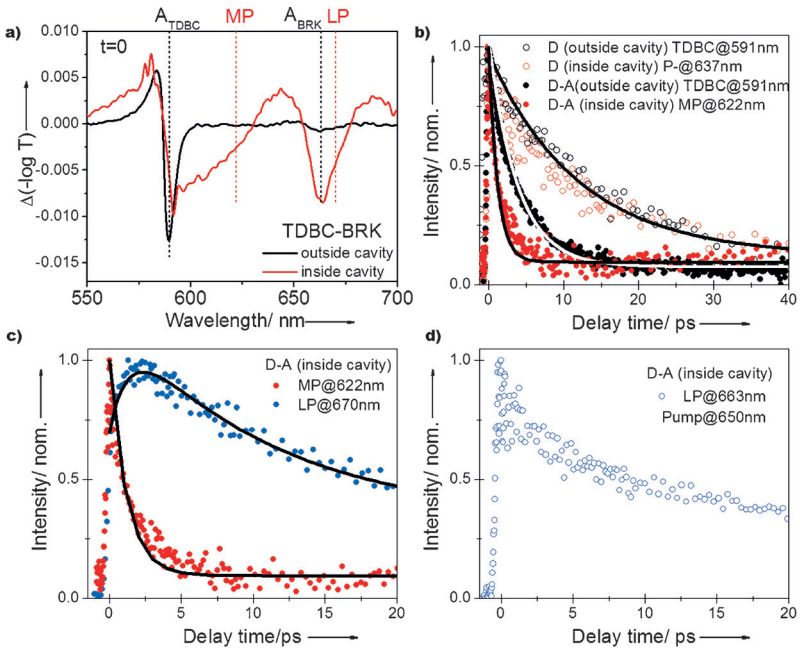

Figure 4. a) Transient absorption spectra of donor–acceptor in the strongly coupled system (red line) and on top of a 30 nm Ag film (black line) with pump wavelength at 530 nm. The black dash lines correspond to the TDBC and BRK absorption maximum and the red dash lines correspond to MP and LP. b) The decay kinetics of donor only outside cavity at TDBC absorption maximum 591 nm (black open circles), of P– in the strongly coupled system at 637 nm (red open circles), of the donor–acceptor (1:0.3) outside cavity at the TDBC absorption maximum 591 nm (black solid circles) and of MP in the strongly coupled system at 622 nm (red solid circles). c) The dynamics recorded at different wavelengths for the strongly coupled donor–acceptor (1:0.3) showing the decay of the signal at wavelengths where MP absorbs and the rise of the LP population. d) Transient dynamics recorded at 663 nm for coupled donor–acceptor (1:0.3) with pump wavelength at 650 nm. The solid lines overlapping the data points in (b) and (c) are the exponential fits according to the method described in the Supporting Information.

transfer rates $R_{ET}=k_{ET}[A]$ can be extracted since $R_{ET}=1/\tau_{DA}-1/\tau_{D}$ and it is much faster in the strongly coupled system ($0.68\times10^{12}\,s^{-1}$) than outside the cavity ($0.10\times10^{12}\,s^{-1}$) under these experimental conditions. The shorter decay lifetimes in the presence of the acceptor are a direct evidence of non-radiative energy transfer in both the strongly coupled system and the normal case outside the cavity. Since [A] is the same outside the cavity and in the strong coupling case, it is the energy transfer rate constant in the cavity k_{ET}^{C} that is enhanced by a factor of seven as compared to that outsidek_{ET}.

In addition, the strongly coupled system should also display the flow of energy from the upper hybrid states to the lowest one due to the different Hopfield coefficients associated with each hybrid state. Indeed this is the case as can be seen in Figure 4c where the time profiles at the wavelengths where LP and MP absorb are compared. As the LP signal rises, the MP decays with matching rates. The corresponding spectral evolution is shown in Figure S3c. When the excitation wavelength is changed to 650 nm (Figure 4d) at the edge of the LP absorption band, no rise in the LP population is seen as expected in the absence of energy transfer. Importantly the lifetime of LP in both cases is about 11 ps. The above experiments were carried out at donor–acceptor ratio of 1:0.3. At higher acceptor concentrations, that is, when the acceptor is more and more strongly hybridized with the donor and cavity photon, the energy transfer dynamics are so fast that it is beyond the limit of our temporal resolution and at least 10 times faster than outside the cavity for the same conditions. Although we excited directly into UP at 530 nm, it decays to MP faster than our time resolution (ca. 150 fs).

The enhanced energy transfer rate constant in the strongly coupled system will lead to an increase in the energy transfer efficiency η_{ET}^{C} and therefore in the efficiency of emission η_{EM}^{C} of the acceptor state upon excitation of the donor since, [Eq. (1)]

$$\eta_{EM}^{C}=\eta_{ET}^{C}\cdot\Phi_{LP}=\frac{k_{ET}^{C}[A]}{k_{r}^{C}+k_{nr}^{C}+k_{ET}^{C}[A]}\cdot\Phi_{LP} \qquad (1)$$

where Φ_{LP} is the emission quantum efficiency of the acceptor state, k_{r}^{C} and k_{nr}^{C} are the radiative and non-radiative decay rate constants of the donor state. Although we don't know Φ_{LP}, we can compare the efficiency of energy transfer outside the cavity η_{ET} with that under strong coupling η_{ET}^{C}. Because $k_{r}\ll k_{nr}$ for both the donor and acceptor whether strongly coupled or not, the effect of seven-fold increase in the energy transfer rate constant should have an equivalent effect on the energy transfer efficiency as can be seen from Equation (1). We estimate that the efficiency increases from $\eta_{ET}\approx0.55$ to $\eta_{ET}^{C}\approx0.90$ from the donor lifetimes in the presence and absence of acceptor. This difference is in qualitative agreement with the emission spectra in Figure 3 where outside the cavity both donor and acceptor fluorescence peaks are observed while in the strongly coupled case the emission is dominated by LP, as discussed earlier. The Förster energy transfer distance must also increase for a given [A] inside the cavity. Using Perrin's equation which treats energy transfer in the absence of molecular diffusion, a rough estimate indicates that the Förster sphere, within which energy transfer can occur, increases by 2.5 in volume.

In our strongly coupled system, the delocalized nature of the hybrid polaritonic states is most likely responsible for enhanced non-radiative energy transfer rate reported herein. This is also what is expected from theoretical studies on energy transport in polaritonic systems,[12,13] and observed for enhanced electronic transport in organic semiconductors under strong coupling.[9] There is evidence that delocalized electronic excited states play a role in photosynthetic light harvesting systems and modifying the traditional incoherent picture of energy transfer.[29] The strongly coupled molecular systems thus provide a convenient way to try to mimic such natural processes by providing a cascade of coherent extended hybrid light-matter states. The optical mode can be tuned to the donor, the acceptor or to a number of molecules simultaneously to create complex systems for energy flow. The present demonstration of efficient energy transfer in such cascades of hybrid states should also be beneficial for solar energy conversion. Light-matter strong coupling thus opens a multitude of possibilities for molecular and materials science.

Acknowledgements

We acknowledge support the ERC through the projects Plasmonics (GA-227557), the International Center for Frontier Research in Chemistry (icFRC, Strasbourg), the ANR Equipex Union (ANR-10-EQPX-52-01), and within the Investissement O'Avenir program ANR-10-IDEX-0002-02 the Labex NIE projects (ANR-11-LABX-0058 NIE) and CSC (ANR-10-LABX-0026 CSC).

Keywords: delocalized state · hybrid polariton · J-aggregate cyanine dye · non-radiative energy transfer · strong coupling

How to cite: *Angew. Chem. Int. Ed.* **2016**, *55*, 6202–6206
Angew. Chem. **2016**, *128*, 6310–6314

[1] P. Törmä, W. L. Barnes, *Rep. Prog. Phys.* **2015**, *78*, 013901.
[2] Y.-W. Hao, H.-Y. Wang, Y. Jiang, Q.-D. Chen, K. Ueno, W.-Q. Wang, H. Misawa, H.-B. Sun, *Angew. Chem.* **2011**, *123*, 7970–7974.
[3] P. Vasa, R. Pomraenke, G. Cirmi, E. De Re, W. Wang, S. Schwieger, D. Leipold, E. Runge, G. Cerullo, C. Lienau, *ACS Nano* **2010**, *4*, 7559–7565.
[4] S. Wang, T. Chervy, J. George, J. A. Hutchison, C. Genet, T. W. Ebbesen, *J. Phys. Chem. Lett.* **2014**, *5*, 1433–1439.
[5] T. Schwartz, J. A. Hutchison, C. Genet, T. W. Ebbesen, *Phys. Rev. Lett.* **2011**, *106*, 196405.
[6] J. A. Hutchison, T. Schwartz, C. Genet, E. Devaux, T. W. Ebbesen, *Angew. Chem. Int. Ed.* **2012**, *51*, 1592–1596; *Angew. Chem.* **2012**, *124*, 1624–1628.
[7] K. S. Daskalakis, S. A. Maier, R. Murray, S. Kéna-Cohen, *Nat. Mater.* **2014**, *13*, 271–278.
[8] J. D. Plumhof, T. Stöferle, L. Mai, U. Scherf, R. F. Mahrt, *Nat. Mater.* **2013**, *13*, 247–252.

[9] E. Orgiu, J. George, J. A. Hutchison, E. Devaux, J. F. Dayen, B. Doudin, F. Stellacci, C. Genet, J. Schachenmayer, C. Genes et al., *Nat. Mater.* **2015**, *14*, 1123 – 1129.
[10] L. Shi, T. K. Hakala, H. T. Rekola, J.-P. Martikainen, R. J. Moerland, P. Törmä, *Phys. Rev. Lett.* **2014**, *112*, 153002.
[11] S. A. Guebrou, C. Symonds, E. Homeyer, J. C. Plenet, Y. N. Gartstein, V. M. Agranovich, J. Bellessa, *Phys. Rev. Lett.* **2012**, *108*, 066401.
[12] J. Feist, F. J. Garcia-Vidal, *Phys. Rev. Lett.* **2015**, *114*, 196402.
[13] J. Schachenmayer, C. Genes, E. Tignone, G. Pupillo, *Phys. Rev. Lett.* **2015**, *114*, 196403.
[14] G. Zengin, M. Wersäll, S. Nilsson, T. J. Antosiewicz, M. Käll, T. Shegai, *Phys. Rev. Lett.* **2015**, *114*, 157401.
[15] S. Wang, A. Mika, J. A. Hutchison, C. Genet, A. Jouaiti, M. W. Hosseini, T. W. Ebbesen, *Nanoscale* **2014**, *6*, 7243.
[16] A. Canaguier-Durand, E. Devaux, J. George, Y. Pang, J. A. Hutchison, T. Schwartz, C. Genet, N. Wilhelms, J.-M. Lehn, T. W. Ebbesen, *Angew. Chem. Int. Ed.* **2013**, *52*, 10533 – 10536; *Angew. Chem.* **2013**, *125*, 10727 – 10730.
[17] D. M. Coles, N. Somaschi, P. Michetti, C. Clark, P. G. Lagoudakis, P. G. Savvidis, D. G. Lidzey, *Nat. Mater.* **2014**, *13*, 712 – 719.
[18] T. Schwartz, J. A. Hutchison, J. Léonard, C. Genet, S. Haacke, T. W. Ebbesen, *ChemPhysChem* **2013**, *14*, 125 – 131.
[19] J. George, S. Wang, T. Chervy, A. Canaguier-Durand, G. Schaeffer, J.-M. Lehn, J. A. Hutchison, C. Genet, T. W. Ebbesen, *Faraday Discuss.* **2015**, *178*, 281 – 294.
[20] G. D. Scholes, *Annu. Rev. Phys. Chem.* **2003**, *54*, 57 – 87.
[21] S. I. Yang, R. K. Lammi, J. Seth, J. A. Riggs, T. Arai, D. Kim, D. F. Bocian, D. Holten, J. S. Lindsey, *J. Phys. Chem. B* **1998**, *102*, 9426 – 9436.
[22] P. Andrew, W. L. Barnes, *Science* **2000**, *290*, 785 – 788.
[23] S. Götzinger, L. d. S. Menezes, A. Mazzei, S. Kühn, V. Sandoghdar, O. Benson, *Nano Lett.* **2006**, *6*, 151 – 1154.
[24] C. Blum, N. Zijlstra, A. Lagendijk, M. Wubs, A. P. Mosk, V. Subramaniam, W. L. Vos, *Phys. Rev. Lett.* **2012**, *109*, 203601.
[25] a) A. Konrad, M. Metzger, A. M. Kern, M. Brecht, A. J. Meixner, *Nanoscale* **2015**, *7*, 10204 – 10209; b) P. Ghenuche, J. de Torres, S. B. Moparthi, V. Grigoriev, J. Wenger, *Nano Lett.* **2014**, *14*, 4707 – 4714.
[26] D. G. Lidzey, D. D. C. Bradley, A. Armitage, S. Walker, M. S. Skolnick, *Science* **2000**, *288*, 1620 – 1623.
[27] J. Wainstain, C. Delalande, D. Gendt, M. Voos, J. Bloch, V. Thierry-Mieg, R. Planel, *Phys. Rev. B* **1998**, *58*, 7269 – 7278.
[28] M. Slootsky, X. Liu, V. M. Menon, S. R. Forrest, *Phys. Rev. Lett.* **2014**, *112*, 076401.
[29] G. D. Scholes, G. R. Fleming, *J. Phys. Chem. B* **2000**, *104*, 1854 – 1868.

Received: January 15, 2016
Revised: March 8, 2016
Published online: April 13, 2016

